Effect of Combined Subsurface Structures and Steps on Hyporheic Exchange

AGU ADVANCING EARTH AND SPACE SCIENCE

Water Resources Research

RESEARCH ARTICLE
10.1029/2022WR033991

Effect of Combined Subsurface Structures and Steps on Hyporheic Exchange

M. Tajari[1], M. H. Omid[1], A. A. Dehghani[2], A. N. Ghameshlou[1], and F. Boano[3]

[1]Department of Irrigation and Reclamation Engineering, College of Agriculture and Natural Resources, University of Tehran, Karaj, Iran, [2]Department of Water Engineering, Gorgan University of Agricultural Sciences and Natural Resources, Gorgan, Iran, [3]Department of Environment, Land, and Infrastructure Engineering, Politecnico di Torino, Turin, Italy

Key Points:

- We modeled hyporheic flow induced by steps, L-shaped structures and boxes
- Steps and boxes drive more hyporheic flow, while steps and L-shaped structures have longer residence times
- When different types of structures are deployed together, hyporheic flow and residence times are controlled by steps

Correspondence to:

F. Boano,
fulvio.boano@polito.it

Citation:

Tajari, M., Omid, M. H., Dehghani, A. A., Ghameshlou, A. N., & Boano, F. (2023). Effect of combined subsurface structures and steps on hyporheic exchange. *Water Resources Research*, *59*, e2022WR033991. https://doi.org/10.1029/2022WR033991

Received 30 OCT 2022
Accepted 18 APR 2023

Abstract The deployment of artificial structures in streambeds has been proposed as a way to enhance 21 hyporheic exchange, and numerical models can be used to quantify their effects. In this study, combinations of different structures—that is, boxes, steps and a new type of subsurface structure (L-shaped structure)—were considered to evaluate their potential applicability on river restoration. Flow-3D and COMSOL were applied to simulate surface and subsurface flow, respectively. The performance of the structures was evaluated on the basis of hyporheic flow and residence time distributions. For the structure sizes here considered, results showed for steps (single step, combination of two steps) and L-shaped structures (single L-shaped structure, combination of two L-shaped structures) most hyporheic flowpaths return to the stream after 5 and 2.5 hr, respectively. Instead, shorter residence times (<0.25 hr) were found for boxes (single box, combination of two boxes). For combinations of steps and permeable boxes, the values of hyporheic flow per unit width are higher (0.35 and 0.3 m^2/hr, respectively) than for the combination of L-shaped (0.06 m^2/hr). As a result, the combinations of steps and boxes are more effective in increasing hyporheic flow. However, when subsurface structures are combined with steps the resulting hyporheic exchange is dominated by the steps. Therefore, the combined use of in-stream and subsurface structures separately may increase their benefits for hyporheic exchange, but when steps are the other subsurface structures provide minor advantages.

1. Introduction

The hyporheic zone (HZ) is an area immediately below the river bed where surface and subsurface water mix together (Orghidan, 1959). The HZ is an ecological hotspot and it has been denoted as the river's liver (Fischer et al., 2005) because it causes the attenuation of specific pollutants such as nutrients or organic contaminants. The main feature of the HZ is the vertical water transfer between surface and subsurface flows that moderates fluctuations of water temperature and strongly influences nutrient cycles (Bakke et al., 2020). Hyporheic exchange is characterized by downwelling and upwelling fluxes (Martone et al., 2020) that are determined by variations in hydraulic head, hydraulic conductivity of the porous medium, and bed thickness (Tonina & Buffington, 2009a, 2009b; Vaux, 1968). The combination of these factors will affect the exchange rate, the residence times in the porous medium, the penetration depth of exchange, and the length of the streamlines in the streambed.

Natural river morphologies such as meanders or bedforms induce hyporheic exchange due to differences in hydraulic head on the river bed. However, human management of rivers can also affect hyporheic flow. Flow restoration operations such as constructed riffles (Kasahara & Hill, 2006), cross-vanes (Daniluk et al., 2012); log dams (Lautz & Fanelli, 2008), and in-stream structures (Hester et al., 2016) can improve water quality due to the enhancement of hyporheic exchange. In spite of the positive effects of hyporheic processes on water quality, river restoration is rarely done with the main goal of increasing hyporheic exchange processes (Boulton, 2007; Ward et al., 2011). Studies on the hyporheic flow have focused traditionally on the exchange caused by the natural morphology of rivers: streambed topography (Harvey & Bencala, 1993); pool-riffle morphology (Tonina & Buffington, 2007); bedforms like dunes (Cardenas et al., 2008; Cardenas & Wilson, 2007; Elliott & Brooks, 1997); alternate bars (Marzadri et al., 2010; Monofy & Boano, 2021); and more complex multiscale morphologies (Stonedahl et al., 2010).

In-stream structures are known as one of the modern solutions for river restoration (Neuhaus & Mende, 2021). River restoration is usually implemented for ecological purposes, including increasing the abundance and survival rates of fishes, and usually relies on creating in-stream structures through the placement of log and

boulder structures (Roni et al., 2018). In addition to the ecological aspects of fish habitats, these structures also affect hyporheic exchange. Field studies of in-stream structures showed that structures that generate differences of the water level induce more hyporheic exchange than natural morphologies of the river bed (Hester et al., 2018; Smidt, 2014). Structures that create a hydraulic gradient like steps, cross vanes, constructed step-pool sequences, and logs increase hyporheic fluxes (Gordon et al., 2013). Aiming to increase the exchange rate and residence times of exchanged water, many studies investigated different in-stream structures like river steps (Endreny et al., 2011a, 2011b; Kasahara & Hill, 2006; Wondzell, 2006); channel-spanning logs (Lautz & Fanelli, 2008; Sawyer & Cardenas, 2012); cross-vanes (Crispell & Endreny, 2009; Daniluk et al., 2012; Gordon et al., 2013; Smidt, 2014); step-pool sequences (Kaushal et al., 2008; Rana et al., 2017); channel-spanning structures and weirs (Brooks, 2017; Feng et al., 2022; Hester & Doyle, 2008; Zhou, 2012; Zhou & Endreny, 2013). The effect of structures buried in the bed or subsurface structures on hyporheic exchanges has been also assessed with sheets and pilings (Vaux, 1968); wedge and box subsurface structures with different hydraulic conductivities (Ward et al., 2011); boxes or blocks with different hydraulic conductivities (Herzog et al., 2016); low conductivity triangular blocks (Herzog, 2017; Herzog et al., 2018); low and high conductivity blocks (Brooks, 2017; Hester et al., 2018), plunge-pool structures (Bakke et al., 2020; Peter et al., 2019). Subsurface structures have advantages like fewer alterations of the surface topography of the stream (including erosion in ponds and steep slopes downstream of cross vanes) (Ward et al., 2011). The most common subsurface structures are boxes or blocks, which usually feature a combination of gravel and an occluding layer, and are buried in the river bed (Bakke et al., 2020).

In-stream structures can increase downwelling fluxes, but increasing hyporheic exchange fluxes alone may not result in improved reach-scale water quality. Several studies have emphasized the importance of matching hyporheic residence times to reaction timescales of interest to optimize contaminant attenuation (Herzog, 2017; Herzog et al., 2018; Hester et al., 2018). Usually, the study of the use of structures has been focused on the analysis of one single element, but to our knowledge there are no precedents in the analysis of the combined effect of in-stream and buried structures over hyporheic exchange. However, the installation of multiple structures can determine interactions between the individual flow fields, with potential alterations of hyporheic exchange fluxes and residence times.

This study relies on numerical modeling to analyze the influence of alternative combinations of structures in rivers on hyporheic flows. The objectives of this study are: (a) to assess the effect of variations in the penetration depth of single steps and combinations of steps on hyporheic exchange; (b) to investigate the influence of different sizes of boxes and combinations of boxes on hyporheic exchange; (c) to assess the effect of variations of size of single and multiple L-shaped structures on hyporheic exchange, and to compare boxes and L-shaped structures; (d) to investigate the influence of combinations of steps and subsurface structures on hyporheic exchange; (e) to compare the different influence of permeable and impermeable subsurface structures on hyporheic exchange. In our study, instead of the analysis of a simple structure, a set of combined in-stream and buried structures were tested, including an innovative shape (L-shape). The L-shaped buried structure can have strong practical implications as it needs less than half of the material for its construction than a box. This type of combined structure and innovative shapes represents an evolution for favoring hyporheic exchange and understanding their potential can be useful to identify new approaches for improving river quality.

2. Methodology

To model the effect of subsurface and in-stream restoration structures and the influence of the combination of these structures on hyporheic exchange, Flow-3D 11.1 (FLOW-3D Documentation, 2012), and COMSOL Multi-physics (COMSOL, Inc., 2008) were used to simulate surface and subsurface flow, respectively. The model is designed to simulate a small reach of a stream where different surface and subsurface structures are added to study the effect on the hyporheic fluxes.

2.1. Surface and Subsurface Flow Modeling

For each simulation, the model included a computational domain with a 2 m length. A 2D model was built using Flow-3D 11.1 using a uniform mesh with a cell size of 5 mm. Preliminary tests showed that the specific value of surface depth had a negligible influence on the simulated hyporheic exchange, which was mainly controlled by

Table 1
Flow and Sediment Characteristics; $Q_{surface}$ Is Surface Flow Discharge Per Unit Stream Width, y Is Surface Water Depth, S Is Streambed Slope, D_{down} and D_{up} Are the Substrate Thicknesses Downstream and Upstream of the Step, Respectively, β' Is the Forchheimer Coefficient, n Is the Substrate and Structure Porosity, k Is the Substrate Permeability, D_{50} Is Median Diameter of Substrate Sediments

	Q_{Surface} (m^2/h)	y (cm)	S	D_{down} (cm)	D_{up} (cm)
Steps	12.8	2	0	37	42
Combination of two steps	12.8	2	0	37	47
Subsurface structures	14	2	0.01	35	37
Combination of step and subsurface structure	12.8	2	0	37	42
	β' (kg/m^4)	n	k (m^2)	D_{50} (mm)	
Bed	10^8	0.4	10^{-10}	0.3	
Subsurface structure	10^7	0.45	10^{-8}	2.4	

spatial variations in hydraulic conductivity. Hence, a constant stream depth of 2 cm above the streambed was used for the upstream and downstream boundary conditions.

The bottom of the model domain was specified as a no-flow boundary. The depth and the slope of the substrate were different depending on the type of structure (Table 1). Specifically, a slope of 1% was adopted when simulating subsurface structures below a flat streambed. This slope value is within the range of Herzog (2017)'s study, which reports values from 0.1% to 2% for urban streams. On the other hand, when a non-flat streambed was considered (i.e., in the presence of step, even in combination with other structures) the surface water profile is mainly controlled by the step height and the slope was hence set to zero.

After simulating flow in the surface domain had stabilized, the results of the total hydraulic head above the streambed were converted to dynamic pressure and then imported into the COMSOL model of subsurface flow. We modeled flow in the porous substrate with the Forchheimer equation. This equation is needed when flow in the substrate is non-Darcian, which corresponds to values of pore Reynolds number ($\frac{V_{\text{pore}} D_{50}}{\upsilon}$) close to or higher than unity (e.g., >0.7–2.3; Kececioglu & Jiang, 1994), where v_{pore} is the pore water velocity (m/s), D_{50} is the average equivalent spherical diameter of the particles of the porous medium (m), and υ is kinematic viscosity of water (m^2/s):

$$-\nabla_p = A|u_{\text{bulk}}|\mu\frac{(1-n)^2}{n^3} + B|u_{\text{bulk}}|^2\rho\frac{(1-n)}{n^3} \quad (1)$$

where u_{bulk} is the apparent bulk velocity (i.e., the volume flux of fluid through the unit area of the material, m/s), ∇_p is the pressure gradient in real space within the porous material, n is porosity, and

$$A = \frac{\alpha}{D_{50}^2}\ B = \frac{\beta}{D_{50}} \quad (2)$$

where α is a constant, typically around 180, β is a roughness factor typically ranging between 1.8 and 4.0 (representing smooth particles through rough fibers). The pore Reynolds number was later calculated and found to reach values higher than one, confirming the need to apply the Forchheimer approach for a more accurate representation of the flow field. For all simulations, boundaries at the streambed surface as well as upstream and downstream boundaries were defined as open boundaries.

2.2. Structure Geometry

Several sets of combinations of structures were tested (Table 2). The surface structures were steps with different penetration depths and different combinations of steps. The subsurface structures were boxes and L-shaped structures with different sizes. Steps were always treated as impermeable but the subsurface structures were considered both permeable and impermeable. In all cases, homogeneous and isotropic permeability was used for the rest of the streambed substrate. Values of the permeability (k) and Forchheimer coefficients (β') are presented in Table 1.

Table 2
Geometrical Characteristics of the Considered Structures

Steps			Boxes and L-shaped subsurface structures		
	H_1 (cm)	H_2 (cm)		H (cm)	L (cm)
$S_{0.5}$	8	3	$B_{0.5}$, $L_{0.5}$	3	10.5
S_1	11	6	B_1, L_1, L_{1r}	6	21
S_2	17	12	B_2, L_2	12	42
Combinations of two steps			**Combinations of two boxes or two L-shaped structures**		
	L1 (cm)	H1 (cm)	H2 (cm)		L1 (cm)	H (cm)	L (cm)
S_1-S_1	20	11	6	B_1-B_1, L_1-L_1	20	6	21
$(S_1$-$S_1)'$	10	11	6	$(B_1$-$B_1)'$, $(L_1$-$L_1)'$	10	6	21
Combinations of steps and box or L-shaped subsurface structures							L_1 (cm)
$S_{0.5}$-$L_{0.5}$							20
S_1-L_1							20
S_2-L_2							20
S_1-B_1							20
S_1-L_{1r}							20

Three different penetration depths of step ($S_{0.5}$, S_1, and S_2) were studied to evaluate the effect of the step configuration, and two combinations of steps, (S_1-S_1) and (S_1-S_1)′, were considered to verify the influence of multiple steps on hyporheic exchange. Also, the simulations included three different dimensions for boxes ($B_{0.5}$, B_1, and B_2), and L-shaped structures ($L_{0.5}$, L_1, and L_2) to evaluate the effect of the size of subsurface structures. Moreover, to analyze the influence of two subsurface structures next to each other, combinations of (B_1-B_1), (B_1-B_1)′, (L_1-L_1), and (L_1-L_1)′ were studied (Table 2 and Figure 1). Finally, the effect of the direction of the L-shaped structure was analyzed with a simulation (L_{1r}) that was identical to L_1 but with the structure flipped along the horizontal direction.

2.3. Calculating Hyporheic Exchange Flow and Residence Time Distributions

The hyporheic exchange flow was calculated through the integration of the downwelling flux over the streambed boundary. The resulting hyporheic exchange flow represents the exchanged volume of water per unit of time and unit stream width.

The effect of the structures on the residence times of hyporheic flow was quantified by simulating the transport of a conservative tracer. A unit tracer concentration was assigned at the inflow boundaries, and the initial concentration in the streambed was set to zero. Residence time distributions (RTDs) were obtained by normalizing the tracer outflux from the streambed for each time step of the simulation with the total tracer influx. The latter value was obtained from the last time step of the simulation as it was verified that the tracer influx reached a stable value after the first time steps. The resulting RTDs were recorded with a uniform time step of 100 s.

In the present study, surface flow simulations with Flow-3D with a spatial resolution of 5 mm required 1–2 hr before the flow to become stable and the results could be acceptable. Modeling subsurface flow with COMSOL with a spatial resolution of 4.6–50 mm was much faster (i.e., some minutes depending on the considered case).

3. Results

3.1. Flow Fields

3.1.1. Steps

The two consecutive steps (S_1-S_1) generate downwelling streamlines upstream of the first step followed by two distinct paths (Figure 2a). Some streamlines return to surface flow downstream of the first step while other ones

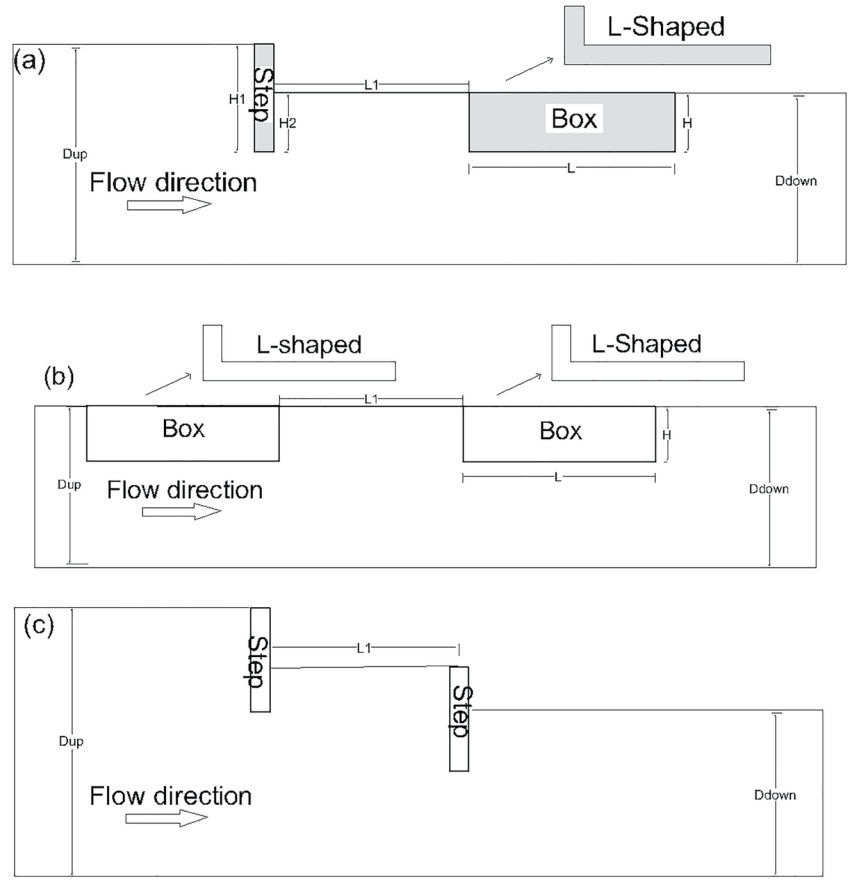

Figure 1. Geometrical characteristics of structures: (a) combination of steps and subsurface structures, where H1 and H2 are the upstream and downstream penetration depths of the step, respectively, L1 is the distance between two structures, L and H are the length and the height of subsurface structure; (b) combination of two subsurface structures; (c) combination of two steps.

flow below the two steps and upwell downstream of the second step. These streamlines tend to bend toward the streambed area between the two steps, which is characterized by a zone of upwelling and downwelling. The result is the presence of a smaller flow cell around each step and a larger flow cell that encompasses both structures.

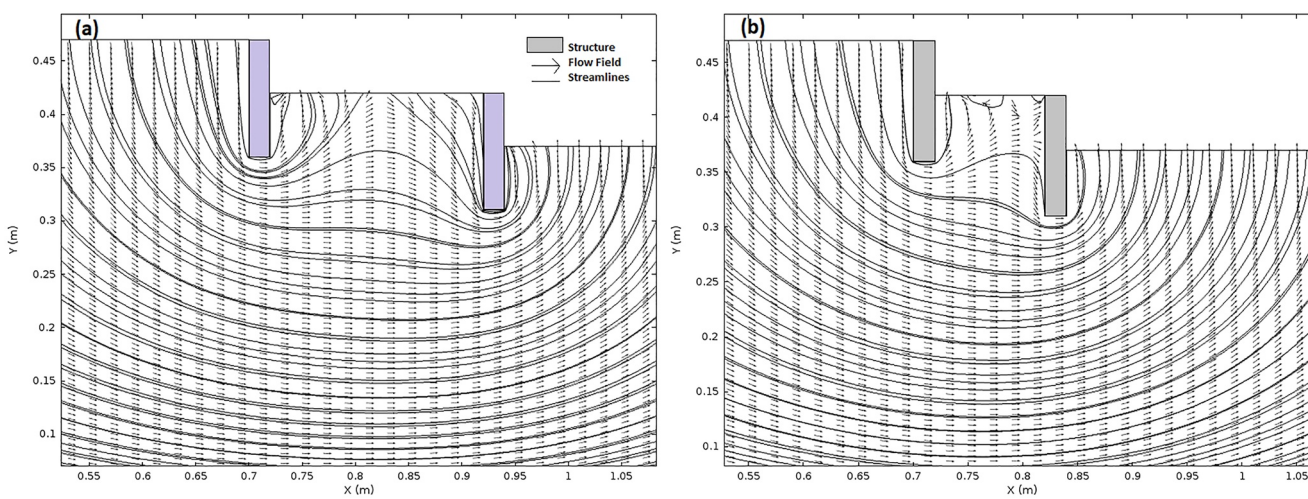

Figure 2. Flow pattern around combinations of steps: (a) S1-S1, (b) (S1-S1)′.

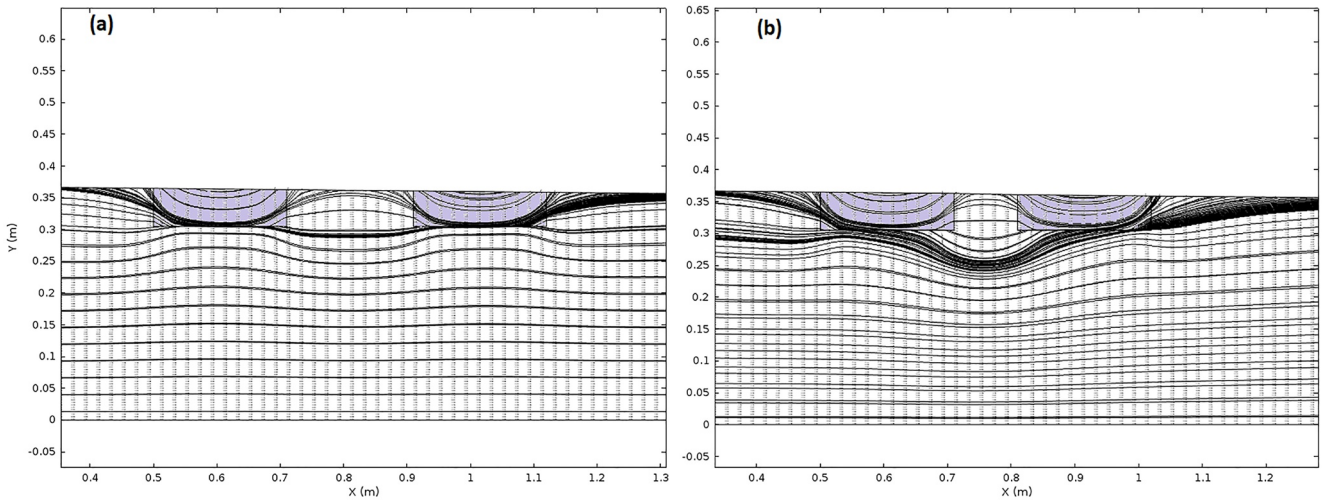

Figure 3. Flow pattern around combinations of permeable boxes: (a) case B_1-B_1, (b) case $(B_1$-$B_1)'$.

When the interval between the two steps decreases for case $(S_1$-$S_1)'$, there is an upwelling area in the middle of the structures (Figure 2b). In this case, the larger flow cell becomes prevalent while the smaller flow cells around the steps tend to disappear.

3.1.2. Box Structures

3.1.2.1. Permeable Boxes

The flow field in the substrate tends to bend toward the box because the structure creates a zone of increased flow capacity due to its higher permeability (Figures 3a and 3b). Downwelling streamlines in the upstream box divide into two parts: some streamlines upwell through the top surface of the box or just downstream of it, while other streamlines flow deeper, pass the interval between the two boxes and upwell at the second box or downstream of it. As a result, there are two small flow cells (near the boxes) and a larger flow cell that flows from the first to the second box (Figure 3a). For the case $(B_1$-$B_1)'$, the streamlines between the two boxes penetrate deeper in the substrate due to the smaller interval between them. Consequently, the larger flow cell becomes deeper while the smaller flow cells around the boxes are similar to those of case B_1-B_1 (Figure 3b).

3.1.2.2. Impermeable Boxes

The impermeable boxes force upwelling upstream of the structure and downwelling downstream of the structure, and no flow cell is present. This pattern occurs because the structure restricts flow in the substrate. Instead, a small flow cell forms between the two boxes for the case of B_1-B_1, surrounded by longitudinal streamlines that tend to bend upward (Figure 4a). For $(B_1$-$B_1)'$, this area is smaller due to the shorter gap between the two boxes (Figure 4b).

3.1.3. L-Shaped Structures

3.1.3.1. Permeable Structures

For case L_1, the flow field in the subsurface tends to bend toward the L-shaped structure. Some streamlines flowing into the structure later return to the substrate, while other ones upwell toward the streambed surface. A pattern of downwelling flow is observed upstream of the L-shaped structure, as water is attracted toward the upstream part of the structure (Figure 5a). For the case of L_{1r}, the flow field is similar to case L_1 with the difference that the flow field is reversed with the inversion of the structure (Figure 5b).

For cases L_1-L_1 and $(L_1$-$L_1)'$, some streamlines flowing out of the first structure are attracted by the second one, Consequently, the smaller flow cells that form around each L-shaped structure are surrounded by a larger flow cell that encompasses both structures (Figures 5c and 5d).

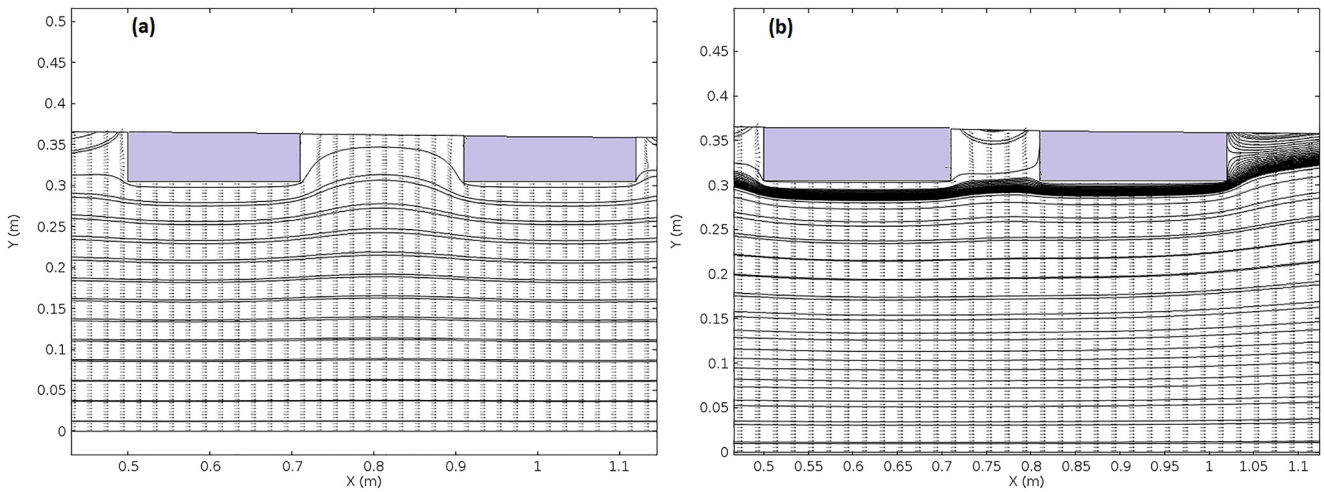

Figure 4. Flow pattern around combinations of impermeable boxes: (a) case B_1-B_1, (b) case $(B_1$-$B_1)'$.

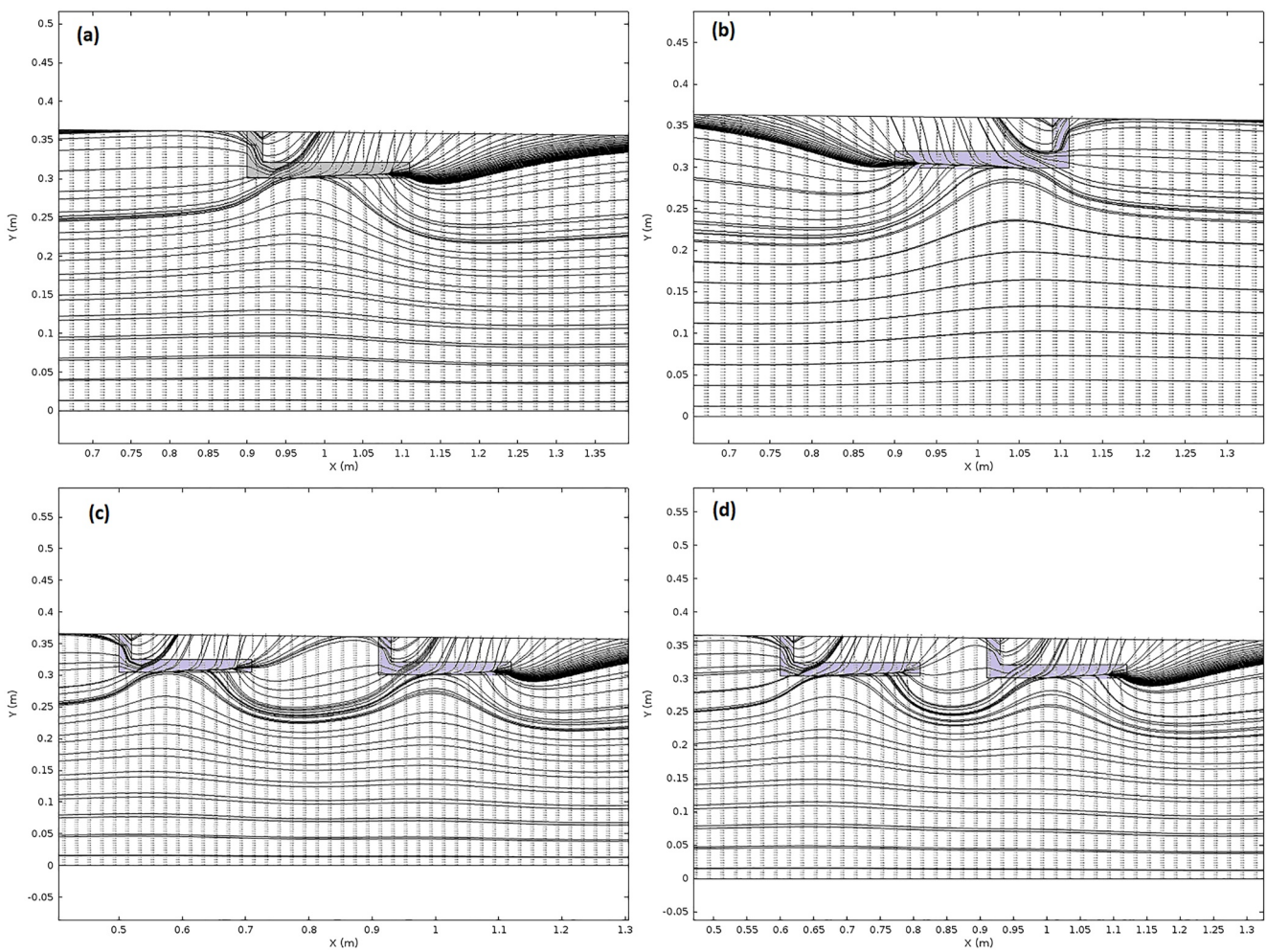

Figure 5. Flow pattern around permeable L-shaped structures: (a) L_1, (b) $L_{1r,}$ (c) L_1-L_1, (d) $(L_1$-$L_1)'$.

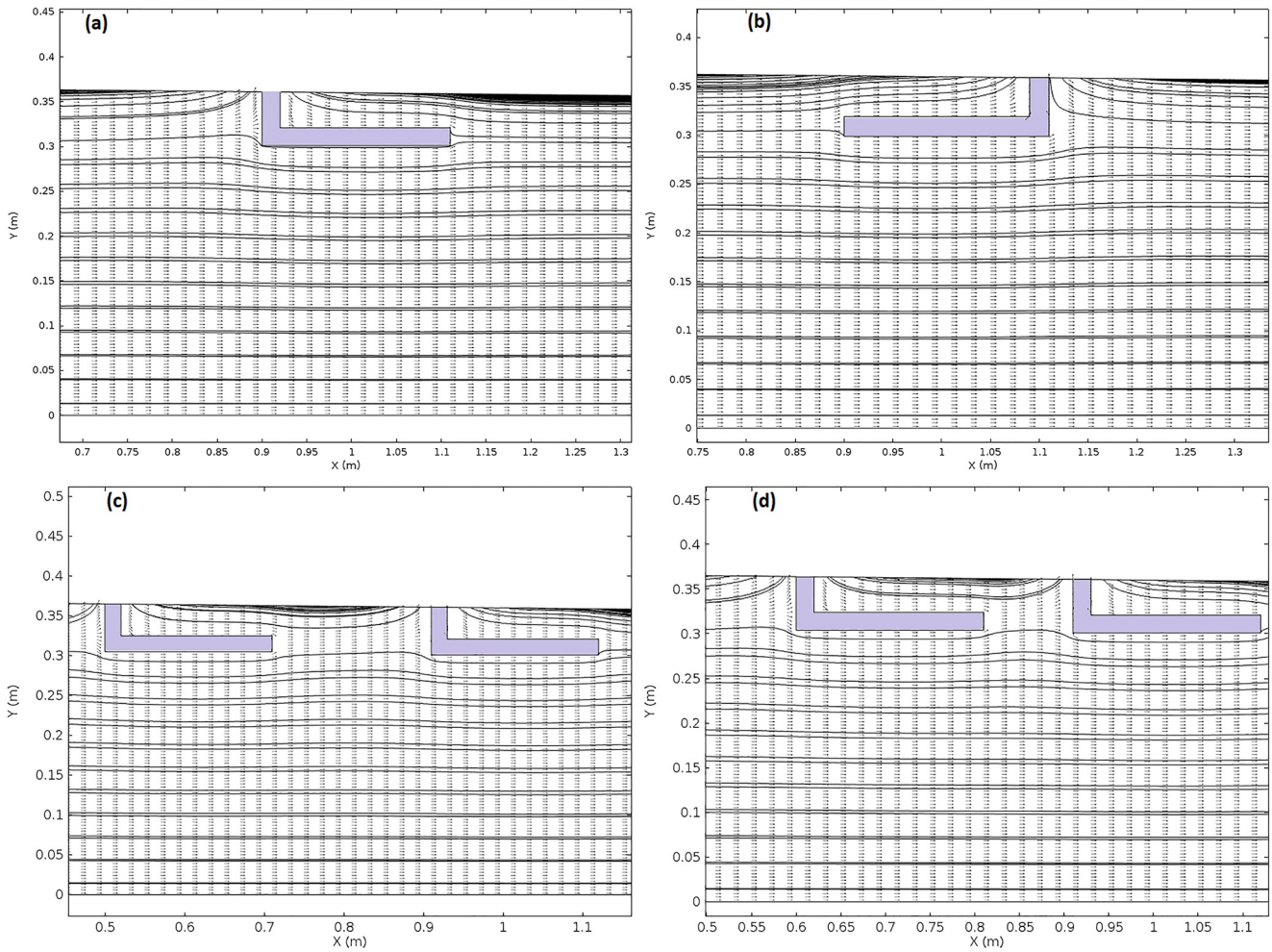

Figure 6. Flow pattern around impermeable L-shaped structures: (a) L_1, (b) $L_{1r,}$ (c) L_1-L_1, (d) $(L_1\text{-}L_1)'$.

3.1.3.2. Impermeable Structures

The impervious L-shaped structures create a characteristic pattern of upwelling and downwelling upstream and downstream of the structure, respectively. The patterns are similar for both L_1 and L_{1r} (Figures 6a and 6b). As for the case of the impermeable boxes, these patterns arise since the structures are an obstacle to the flow field.

For cases of L_1-L_1 and $(L_1\text{-}L_1)'$, the previous pattern can again be observed but the combination of two L-shaped structures creates a flow cell between the two structures. The interval between the structures has a minor effect on the shape of streamlines (Figures 6c and 6d).

3.1.4. Combination of Steps and Subsurface Structures

For a combination of a step and a permeable L-shaped structure, the flow field is mostly influenced by the step while the permeable L-shaped structure has a negligible effect on it (Figure 7a). For a combination of step and impervious structure, the flow field is similar to the previous type with the difference that the impermeable structure behaves like a barrier that diverts the streamlines (Figure 7b). These results suggest that steps exert a major control on hyporheic exchange compared to subsurface boxes and L-shaped structures.

3.2. Hyporheic Flow

3.2.1. Steps

The penetration depth of the step decreases hyporheic flow, as shown by the comparison of cases $S_{0.5}$, $S_{1,}$ and S_2 (Figure 8a). The values of the hyporheic exchange flow per unit stream width are around 0.2 m^2/hr for these cases.

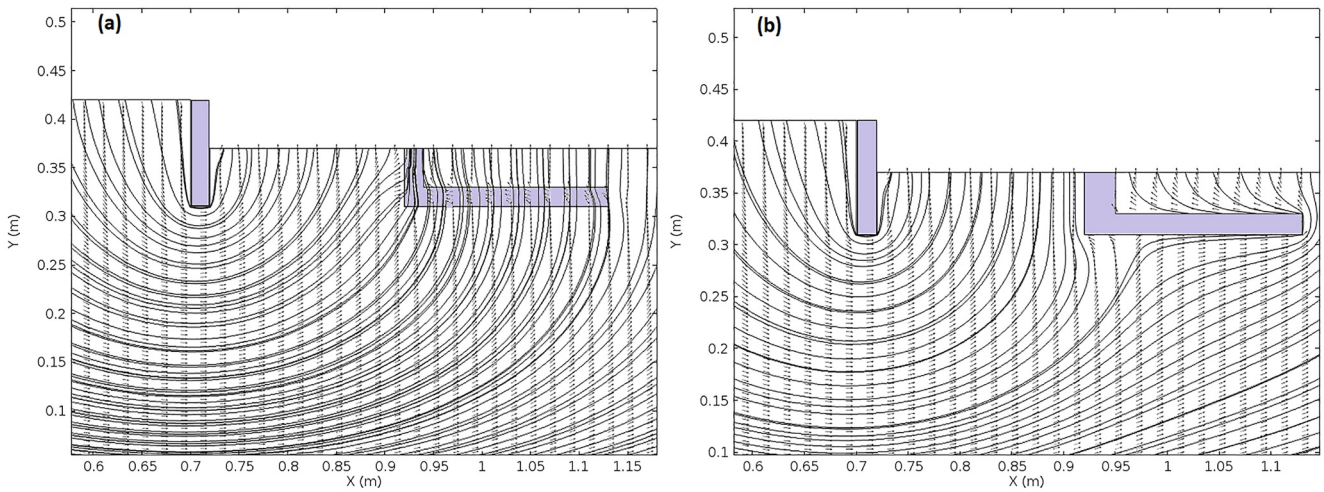

Figure 7. Flow pattern around the combination of step and L-shaped structures (S_1-L_1): (a) permeable L-shaped structure, (b) impermeable L-shaped structure.

The combination of two steps in cases S_1-S_1 and $(S_1$-$S_1)'$ enhances flow to more than 0.3 m^2/hr because these combinations increase the length of the downwelling zone, as shown in Figure 2. However, hyporheic flow with two steps is much less than twice the value for a single step. This result indicates that the interaction between the structures reduces the potential for the exchange of each step.

3.2.2. Boxes

A larger structure generates higher hyporheic flow (compare cases $B_{0.5}$, B_1, and B_2 in Figure 8b). Permeable boxes result in much higher flow compared to impervious boxes. For permeable boxes, hyporheic flow for cases of $B_{0.5}$, B_1, and B_2 are 0.07, 0.15, and 0.3 m^2/hr, respectively, while impervious boxes have little hyporheic flow (0.0007, 0.0014, and 0.0029 m^2/hr). By combining two boxes, the amount of hyporheic flow is almost twice than for a

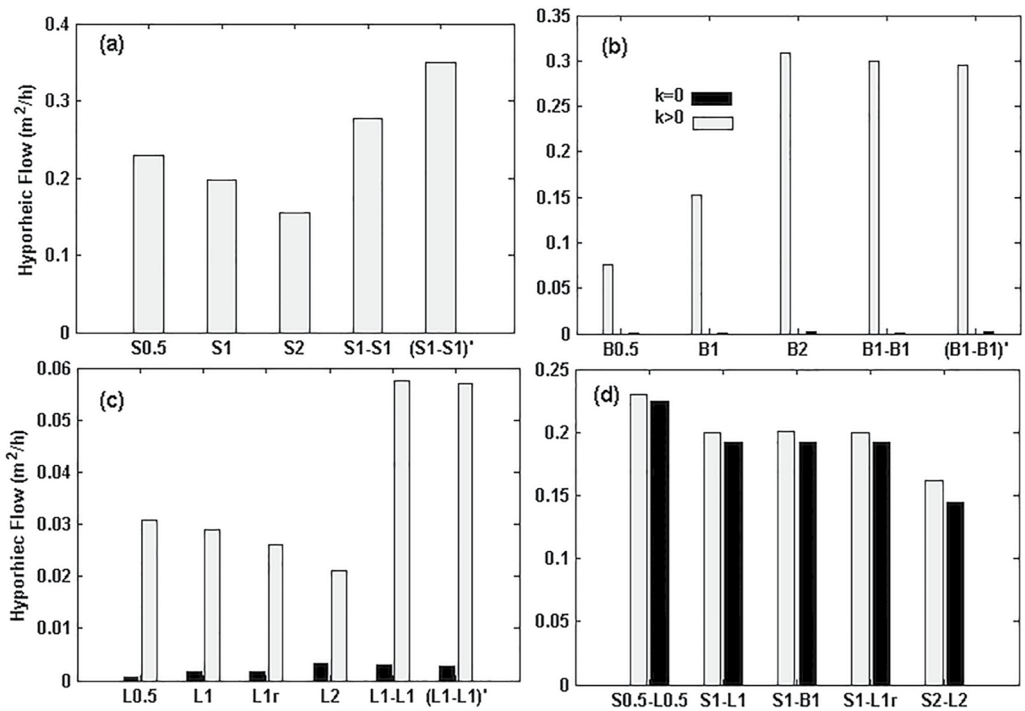

Figure 8. Hyporheic exchange flow: (a) steps, (b) boxes, (c) L-shaped structures, (d) combinations of step and L-shaped structures.

single box (Figure 8b). The hyporheic flow for B_2 and the combination of two smaller boxes (B_1-B_1) is almost the same. It means that doubling the size of the structure and combining two boxes have the same effect on the amount of hyporheic flow. Finally, the comparison between (B_1-B_1) and (B_1-B_1)′ shows a very small difference in hyporheic flow, which suggests that the distance between boxes does not influence the magnitude of water exchange.

3.2.3. L-Shaped Structures

For permeable L-shaped structures, increasing structure size from case $L_{0.5}$ to case L_2 creates slightly lower hyporheic flow (Figure 8c). Also, L-shaped structures induce a limited amount of downwelling flow, and some streamlines entering the substrate remain in the subsurface and do not participate in hyporheic exchange (refer to Section 3.1.3), which results in small values of hyporheic flow compared to steps and boxes.

Combinations of L-shaped structures increase hyporheic flow compared to a single structure of the same size. The hyporheic flow of the combinations is almost twice the value for a single one (L_1), which suggests that the interactions between the small flow cells of the single structures have a minor influence on the rate of water exchange. The difference in flow between cases L_1 and case L_{1r} is small, with a slightly lower flow for L_r. For impermeable structures, increasing size and combining multiple structures enhance hyporheic flow, but values of fluxes are insignificant compared to the case of permeable structures.

3.2.4. Combination of Steps and Subsurface Structures

For the combination of steps and subsurface structure, the hyporheic flow value is similar to the flow values of single steps (Figure 8d). In fact, steps have the main role in driving hyporheic exchange when combined with other structures (see Section 3.1.4), so the flow magnitude for the combination of a step and a permeable structure is almost equal to the corresponding combination of a step and an impervious structure.

Increased structure size decreases flux as shown by the comparison of cases $S_{0.5}$-$L_{0.5}$, S_1-L_1 and S_2-L_2. However, a variation of size has little effect on the values of hyporheic flow, which range from 0.2 to 0.25 m^2/hr for these cases.

When L-shaped structures are replaced by boxes in the combination with steps, the hyporheic flow is almost identical (e.g., for S_1-B_1 and S_1-L_1). The hyporheic exchange flows of the boxes and L-shaped structures are different, confirming that the hyporheic flow is controlled by the presence of the steps even when the other structures are included.

3.3. Residence Time Distributions

3.3.1. Steps

RTDs are sensitive to variations in structure penetration depth, and residence times generally increase as structure penetration depth increases because streamlines become longer (Figure 9a). For cases $S_{0.5}$, S_1, and S_2, RT_{50} is 0.23, 0.33, and 0.59 hr, and RT_{80} is 1.22, 1.36, and 1.97 hr, respectively. When two steps are considered (cases S_1-S_1 and (S_1-S_1)′), there is a very small increase in residence time for S_1-S_1, while for (S_1-S_1)′ the residence times are even smaller than for a single structure (case S_1).

3.3.2. Boxes

For permeable boxes, streamlines become longer for larger structure sizes, so residence times increase, even though these residence times are much shorter than those obtained for the steps (Figure 9b). For cases $B_{0.5}$, B_1, and B_2, RT_{50} is 0.019, 0.035, and 0.065 hr, and RT_{80} is 0.046, 0.07, and 0.11 hr, respectively. These values show that a two-fold increase in box size (e.g., compare $B_{0.5}$ and B_1) leads to increases in RT_{50} and RT_{80} of a factor of approximately 1.8 and 1.5, respectively. The presence of two structures causes the replication of the flow pattern of a single box, so for cases B_1-B_1 and (B_1-B_1) the RTDs are almost identical to B_1. For the case of impermeable boxes, the RTD cannot be determined because almost all downwelling streamlines do not flow back to the stream within the computational domain, and there is no flow cell around the structures (Section 3.1.2).

3.3.3. L-Shaped Structures

Increased structure size enhances the residence times, whose values have the same order of magnitude as those of the steps. However, an important difference is that the RTDs do not reach 100% for large residence times (Figure 9c). This means that a part of the total downwelling flow moves through the substrate and leaves the domain from the

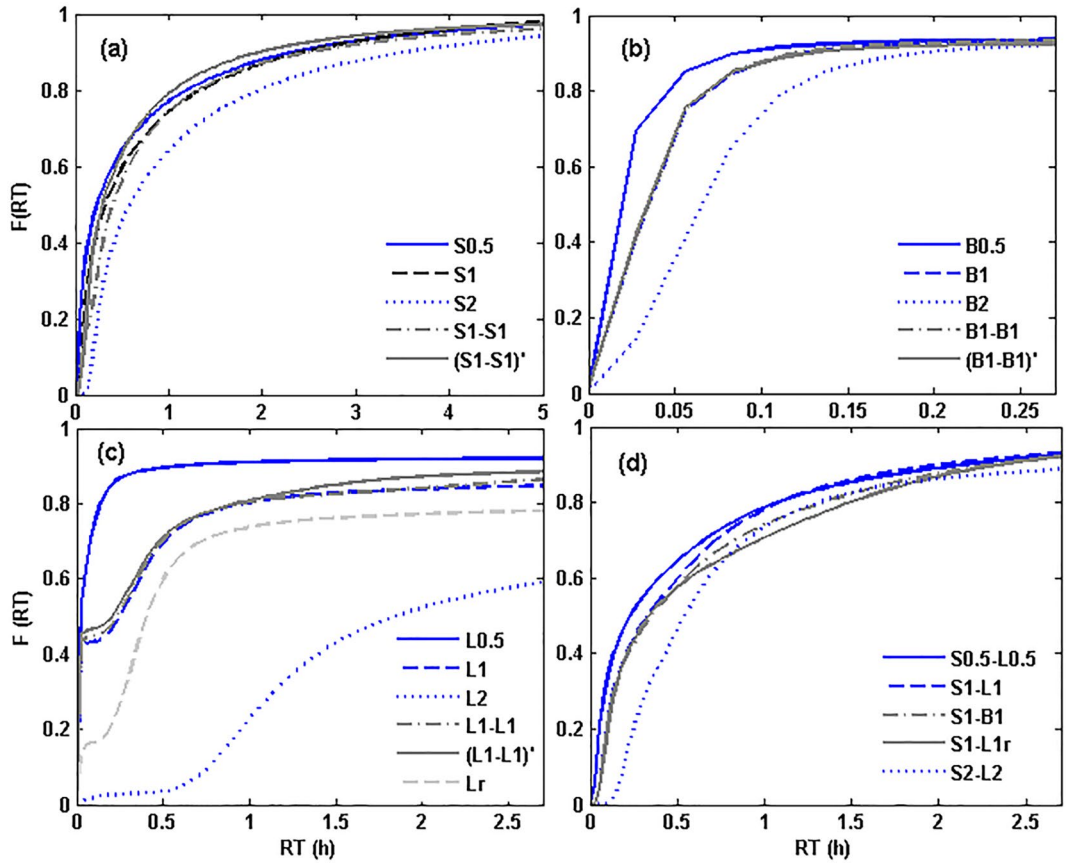

Figure 9. Residence time distributions: (a) steps, (b) permeable boxes, (c) permeable L-shaped structures, (d) combinations of step and subsurface structures.

downstream boundary. In real systems, these streamlines will eventually upwell again at some point downstream (e.g., due to changes in permeability), and this results in residence times that are substantially longer than those of other structures. The presence of two structures causes the replication of the flow pattern, so for cases L_1-L_1 and (L_1-L_1) the RTDs are almost identical to a single structure with the same size (case L_1). For cases L_1, L_1-L_1, and (L_1-L_1)′, almost 50% of the hyporheic flow has very short residence times because the hyporheic flow created by these structures is not very deep. The comparison of L_1 and L_r shows that the reversed structure of L_r exhibits larger residence times, and only 15% of hyporheic flow has a very short residence time (Figure 9c). This indicates that the use of reversed L-shaped structures can be preferred if longer residence times are sought.

3.3.4. Combination of Steps and Subsurface Structures

The residence time increases with larger structure combination size. For the cases of $S_{0.5}$-$L_{0.5}$, S_1-L_1, and S_2-L_2, RT_{50} is 0.23, 0.33, and 0.55 hr, and RT_{80} is 1.08, 1.11, and 1.33 hr, respectively. These values show that the combined structures result in RTDs that are similar to RTDs of steps, particularly for median residence times (Figure 9d). However, the slightly lower values of RT_{80} compared to those of steps alone indicate a small influence of the additional L-shaped structure on the tail of the RTD.

For cases S_1-L_1, S_1-L_{1r}, and S_1-B_1, RTDs are insensitive to changing the type of subsurface structure for residence times below RT_{50}, while for larger times a small difference between RTDs of the three cases (e.g., RT_{80} of S_1-L_{1r} > RT_{80} of S_1-B_1 > RT_{80} of S_1-L_1). Despite these small differences, these results confirm that the RTD induced by the combination of steps and other structures is mostly affected by the RTD of steps.

4. Discussion and Conclusions

Steps and L-shaped structures generate downwelling flow that returns to the stream after longer times (between 5 and 2.5 hr, respectively) compared with boxes (<0.25 hr). While steps have apparently the longest residence

times, part of the streamlines induced by L-shaped did not return to surface flow within the simulation domain and stayed in the substrate for longer distances. These streamlines may actually have very long residence times that can be very effective for reactions in the subsurface but our modeling approach cannot take into account these effects. For steps and permeable boxes, the values of hyporheic flow are high and close to each other, while L-shaped structures drive less hyporheic flow. As a result, steps and boxes are more effective in increasing hyporheic flow.

Previous studies (Ward et al., 2011) focused on single, bigger boxes (0.01–20 m length and 0.03–2.97 m height), obtaining residence times ranging between 27 and 2,777 hr. The difference between residence times of our study is related to the size of the domain and to their lower hydraulic conductivity (5.0×10^{-5} m/s, corresponding to a permeability of approximatively 5×10^{-12} m^2) that reduced flow velocity in the substrate and induced purely Darcian flow.

Feng et al. (2022) considered the effect of a weir, whose geometry partially resembles the one of a step. Their results showed that the hyporheic flow and the maximum solute penetration depth generally increased with the weir height outside sediment, and hyporheic flow was sensitive to changes in permeability between 10^{-8} and 10^{-10} m^2, with negligible hyporheic flow below 10^{-10} m^2.

The structure in Feng et al. (2022) kept a constant penetration depth of the impermeable sheet pile, but the overall sheet pile was lengthened so that greater lengths extended into the surface water column (i.e., greater height above streambed). In contrast, the results of this study show a reduction of hyporheic flow with increasing penetration depth of step and the presence of hyporheic flow even at low permeability. In the present study, the increase in penetration depth rather than in step height is the reason for the difference with the results of Feng et al. (2022).

The type of sediment has an important effect on hyporheic flow. Sediments with high porosity generate non-inertial flow within the porous medium and are associated with shorter residence times (Feng et al., 2022). In the present study, due to the considered sediments, non-inertial flow was established in the porous medium close to the surface or in correspondence of structures with high permeability. Even though the chosen hydraulic properties of the sediments are common, the results of this study have been obtained assuming homogenous conditions. Heterogeneous sediment properties are common in natural settings (Sebok et al., 2015). Salehin et al., 2004 and Tonina and Buffington (2009a, 2009b) found that heterogeneity increases the hyporheic exchange flux. Whereas heterogeneity increases the tortuosity of the streamlines, thus increasing the residence time of short streamlines, it reduces long residence times with respect to the homogeneous case because of compression of the HZ (Tonina et al., 2016). In combination with sediment heterogeneity, spatial variations in the subsurface flow field can also be caused by net groundwater upwelling in gaining reaches (e.g., Gomez-Velez et al., 2014), a factor that was not considered in the present work.

According to the results of hyporheic flow and RTDs of the structures, steps are more effective than subsurface structures (boxes and L-shaped structures). In fact, steps create more hyporheic flow and longer residence times. After the comparison of five cases of steps, the use of the combination S_1-S_1 and the single structure S_2 are recommended to have more hyporheic flow and longer residence times, respectively. As expected, permeable and impervious structures exhibited different behaviors. The results of our study show that impermeable subsurface structures induce less hyporheic flow than permeable structures, so the use of permeable subsurface structures instead of impervious structures is recommended. As we anticipated, the combination of two steps or two subsurface structures creates more hyporheic flow. While we expected larger subsurface structures to drive more hyporheic exchange, this was not true in the case of L-shaped structures. The comparison between boxes and L-shaped structures revealed that boxes induce more hyporheic flow and L-shaped structures have longer residence times. To attenuate pollution, long residence times of hyporheic flow in the substrate are necessary (Peter et al., 2019), and L-shaped structures can thus be more effective than boxes.

The choice of the size of the structure can help to obtain the desired values of exchange flow and residence times to enhance nutrient reactions and/or oxygen supply in the HZ, and this study improves our understanding of how the structure size affects hyporheic exchange. When the size of the permeable boxes is increased a larger portion of the sediment is affected by hyporheic exchange and hyporheic flow increases, in agreement with the results of Ward et al. (2011). An opposite behavior has been found for permeable L-shaped structures. When steps are combined with subsurface structures, hyporheic flow is mostly affected by the step. Hence, increasing the size of the combined structures decreases hyporheic flow because the overall exchange is controlled by the step. For

impervious L-shaped structures and boxes, the hyporheic flow increases with the size of the structure. However, hyporheic flow for these structures is very low and negligible, and their use for hyporheic flow control is thus not recommended. Further studies are needed to deal with the complexity of real stream environments (e.g., flow variability, sediment heterogeneity) and to provide design guidelines for stream restoration structures that are effective in enhancing hyporheic exchange.

Data Availability Statement

Data generated in this study is available at https://doi.org/10.5281/zenodo.7825332.

Acknowledgments
This research was supported by Iran National Science Foundation (INSF) as a project with number 99023287 and the title Effects of in-stream structures in tandem with local river bed hydraulic-conductivity modification on hyporheic flow characteristics.

References

Bakke, P. D., Hrachovec, M., & Lynch, K. D. (2020). Hyporheic process restoration: Design and performance of an engineered streambed. *Water*, *12*(2), 425. https://doi.org/10.3390/w12020425

Boulton, A. J. (2007). Hyporheic rehabilitation in rivers: Restoring vertical connectivity. *Freshwater Biology*, *52*(4), 632–650. https://doi.org/10.1111/j.1365-2427.2006.01710.x

Brooks, K. E. (2017). Comparing reach scale hyporheic exchange and denitrification induced by instream restoration structures and natural streambed morphology. Thesis submitted to the faculty of the Virginia Polytechnic Institute and State University in partial fulfillment for the requirements for the degree of Master of Science in Environmental Engineering.

Cardenas, M. B., & Wilson, J. L. (2007). Effects of current–bed form induced fluid flow on the thermal regime of sediments. *Water Resources Research*, *43*(8), W08431. https://doi.org/10.1029/2006WR005343

Cardenas, M. B., Wilson, J. L., & Haggerty, R. (2008). Residence time of bedform-driven hyporheic exchange. *Advances in Water Resources*, *31*(10), 1382–1386. https://doi.org/10.1016/j.advwatres.2008.07.006

COMSOL, Inc. (2008). COMSOL multiphysics, Version 3.5. User's guide and reference guide.

Crispell, J. K., & Endreny, T. A. (2009). Hyporheic exchange flow around constructed in-channel structures and implications for restoration design. *Hydrological Processes*, *23*(8), 1158–1168. https://doi.org/10.1002/hyp.7230

Daniluk, T. L., Lautz, L. K., Gordon, R. P., & Endreny, T. A. (2012). Surface water-groundwater interaction at restored streams and associated reference reaches. *Hydrological Processes*, *27*(25), 3730–3746. https://doi.org/10.1002/hyp.9501

Elliott, A. H., & Brooks, N. H. (1997). Transfer of nonsorbing solutes to a streambed with bed forms: Laboratory experiments. *Water Resources Research*, *33*(1), 137–151. https://doi.org/10.1029/96wr02783

Endreny, T., Lautz, L., & Siegel, D. I. (2011a). Hyporheic flow path response to hydraulic jumps at river steps: Flume and hydrodynamic models. *Water Resources Research*, *47*(2). https://doi.org/10.1029/2009WR008631

Endreny, T., Lautz, L., & Siegel, D. I. (2011b). Hyporheic flow path response to hydraulic jumps at river steps: Hydrostatic model simulations. *Water Resources Research*, *47*(2), W02518. https://doi.org/10.1029/2010WR010014

Feng, J., Liu, D., Liu, Y., Li, Y., Li, H., Chen, L., et al. (2022). Hyporheic exchange due to in-stream geomorphic structures. *Journal of Freshwater Ecology*, *37*(1), 221–241. https://doi.org/10.1080/02705060.2022.2034673

Fischer, H., Kloep, F., Wilzcek, S., & Pusch, M. (2005). A river's liver—Microbial processes within the hyporheic zone of a large lowland river. *Biogeochemistry*, *76*(2), 349–371. https://doi.org/10.1007/s10533-005-6896-y

FLOW-3D Documentation. (2012). Flow Science, Inc.

Gomez-Velez, J. D., Krause, S., & Wilson, J. L. (2014). Effect of low-permeability layers on spatial patterns of hyporheic exchange and groundwater upwelling. *Water Resources Research*, *50*(6), 5196–5215. https://doi.org/10.1002/2013wr015054

Gordon, R. P., Lautz, L. K., & Daniluk, T. L. (2013). Spatial patterns of hyporheic exchange and biogeochemical cycling around cross-vane restoration structures: Implications for stream restoration design. *Water Resources Research*, *49*(4), 2040–2055. https://doi.org/10.1002/wrcr.20185

Harvey, J. W., & Bencala, K. E. (1993). The effect of streambed topography on surface-subsurface water exchange in mountain catchments. *Water Resources Research*, *29*(1), 89–98. https://doi.org/10.1029/92wr01960

Herzog, S. P. (2017). Biohydrochemical enhancements for stearmwater treatment: Engineered hypoheic zones to increase hyporheic exchange, control residence times, and improve water quality. Ph. D. thesis, the Faculty and Board of Trustees of the Colorado School of Mines in partial fulfillment of the requirements.

Herzog, S. P., Higgins, C. P., & McCray, J. E. (2016). Engineered streambeds for induced hyporheic flow: Enhanced removal of nutrients, pathogens, and metals from urban streams. *Journal of Environment and Engineering*, *142*(1), 0001012. https://doi.org/10.1061/(asce)ee.1943-7870

Herzog, S. P., Higgins, C. P., Singha, K., & McCray, J. E. (2018). Performance of engineered streambeds for inducing hyporheic transient storage and attenuation of resazurin. *Environmental Science & Technology*, *52*(18), 10627–10636. https://doi.org/10.1021/acs.est.8b01145

Hester, E. T., Brooksa, K. E., & Scott, D. T. (2018). Comparing reach scale hyporheic exchange and denitrification induced by instream restoration structures and natural streambed morphology. *Ecological Engineering*, *115*, 105–121. https://doi.org/10.1016/j.ecoleng.2018.01.011

Hester, E. T., & Doyle, M. W. (2008). In-stream geomorphic structures as drivers of hyporheic exchange. *Water Resources Research*, *44*(3), W03417. https://doi.org/10.1029/2006WR005810

Hester, E. T., Hammond, B., & Scott, D. T. (2016). Effects of inset floodplains and hyporheic exchange induced by in-stream structures on nitrate removal in a headwater stream. *Ecological Engineering*, *97*, 452–464. https://doi.org/10.1016/j.ecoleng.2016.10.036

Kasahara, T., & Hill, A. R. (2006). Effects of riffle-step restoration on hyporheic zone chemistry in N-rich lowland streams. *Canadian Journal of Fisheries and Aquatic Sciences*, *63*(1), 120–133. https://doi.org/10.1139/f05-199

Kaushal, S. S., Groffman, P. M., Mayer, P. M., Striz, E., & Gold, A. J. (2008). Effects of stream restoration on denitrification in an urbanizing watershed. *Ecological Applications*, *18*(3), 789–804. https://doi.org/10.1890/07-1159.1

Kececioglu, I., & Jiang, Y. (1994). Flow through porous media of packed spheres saturated with water. *Journal of Fluids Engineering*, *116*(1), 164–170. https://doi.org/10.1115/1.2910229

Lautz, L. K., & Fanelli, R. M. (2008). Seasonal biogeochemical hotspots in the streambed around restoration structures. *Biogeochemistry*, *91*(1), 85–104. https://doi.org/10.1007/s10533-008-9235-2

Martone, I., Gualtieri, C., & Endreny, T. (2020). Characterization of hyporheic exchange drivers and patterns within a low-gradient, first-order, river confluence during low and high flow. *Water*, *12*(3), 649. https://doi.org/10.3390/w12030649

Marzadri, A., Tonina, D., Bellin, A., Vignoli, G., & Tubino, M. (2010). Semianalytical analysis of hyporheic flow induced by alternate bars. *Water Resources Research*, *46*(7), W07531. https://doi.org/10.1029/2009WR008285

Monofy, A., & Boano, F. (2021). The effect of streamflow, ambient groundwater, and sediment anisotropy on hyporheic zone characteristics in alternate bars. *Water Resources Research*, *57*(1), e2019WR025069. https://doi.org/10.1029/2019WR025069

Neuhaus, V., & Mende, M. (2021). Engineered large wood structures in stream restoration projects in Switzerland: Practice-based experiences. *Water*, *13*(18), 2520. https://doi.org/10.3390/w13182520

Orghidan, T. (1959). Ein neuer Lebensraum des unterirdischen Wassers: Der hyporheische Biotop. *Archiv für Hydrobilogie*, *55*, 392–414.

Peter, K. T., Herzog, S., Tian, Z., Wu, C., McCray, J. E., Lynch, K., & Kolodziej, E. P. (2019). Evaluating emerging organic contaminant removal in an engineered hyporheic zone using high resolution mass spectrometry. *Water Research*, *150*, 140–152. https://doi.org/10.1016/j.watres.2018.11.050

Roni, P., Weber, C., & Åberg, U. (2018). A review of approaches for monitoring the effectiveness of regional and national river restoration programs. *North American Journal of Fisheries Management*, *38*, 1170–1186. https://doi.org/10.1002/nafm.10222

Rana, S. M., Scott, D. T., & Hester, E. T. (2017). Effects of in-stream structures and channel flow rate variation on transient storage. *Journal of Hydrology*, *548*, 157–169. https://doi.org/10.1016/j.jhydrol.2017.02.049

Salehin, M., Packman, A. I., & Paradis, M. (2004). Hyporheic exchange with heterogeneous streambeds: Laboratory experiments and modeling. *Water Resources Research*, *40*(11). https://doi.org/10.1029/2003WR002567

Sawyer, A. H., & Cardenas, M. B. (2012). Effect of experimental wood addition on hyporheic exchange and thermal dynamics in a losing meadow stream. *Water Resources Research*, *48*(10), W10537. https://doi.org/10.1029/2011WR011776

Sebok, E., Duque, C., Engesgaard, P., & Boegh, E. (2015). Spatial variability in streambed hydraulic conductivity of contrasting stream morphologies: Channel bend and straight channel. *Hydrological Processes*, *29*(3), 458–472. https://doi.org/10.1002/hyp.10170

Smidt, S. J. (2014). A thesis submitted in partial fulfillment of the requirements for the Master of Science degree in Geoscience in the Graduate College of the University of Iowa.

Stonedahl, S. H., Harvey, J. W., Wörman, A., Salehin, M., & Packman, A. I. (2010). A multiscale model for integrating hyporheic exchange from ripples to meanders. *Water Resources Research*, *46*(12). https://doi.org/10.1029/2009wr008865

Tonina, D., & Buffington, J. M. (2007). Hyporheic exchange in gravel bed-rivers with pool-riffle morphology: Laboratory experiments and three-dimensional modeling. *Water Resources Research*, *43*(1), 1–16. https://doi.org/10.1029/2005wr004328

Tonina, D., & Buffington, J. M. (2009a). Hyporheic exchange in mountain rivers I: Mechanics and environmental effects. *Geography Compass*, *3/3*(3), 1063–1086. https://doi.org/10.1111/j.1749-8198.2009.00226.x

Tonina, D., & Buffington, J. M. (2009b). A three-dimensional model for analyzing the effects of salmon redds on hyporheic exchange and egg pocket habitat. *Canadian Journal of Fisheries and Aquatic Sciences*, *66*(12), 2157–2173. https://doi.org/10.1139/f09-146

Tonina, D., de Barros, F. P. J., Marzadri, A., & Bellin, A. (2016). Does streambed heterogeneity matter for hyporheic residence time distribution in sand-bedded streams? *Advances in Water Resources*, *96*, 120–126. https://doi.org/10.1016/j.advwatres.2016.07.009

Vaux, W. G. (1968). Intragravel flow and interchange of water in a streambed. *Fishery Bulletin of the Fish and Wildlife Service*, *66*(3), 479–489.

Ward, A. S., Gooseff, M. N., & Johnson, P. A. (2011). How can subsurface modifications to hydraulic conductivity be designed as stream restoration structures? Analysis of Vaux's conceptual models to enhance hyporheic exchange. *Water Resources Research*, *47*(8), W08512. https://doi.org/10.1029/2010wr010028

Wondzell, S. M. (2006). Effect of morphology and discharge on hyporheic exchange flows in two small streams in the Cascade Mountains of Oregon, USA. *Hydrological Processes*, *20*(2), 267–287. https://doi.org/10.1002/hyp.5902

Zhou, T. (2012). Characterizing hydrodynamics and hyporheic impacts of river restoration structures. A dissertation submitted in partial fulfillment of the requirements for the Doctor of Philosophy Degree State University of New York College of Environmental Science and Forestry Syracuse.

Zhou, T., & Endreny, T. A. (2013). Reshaping of the hyporheic zone beneath river restoration structures: Flume and hydrodynamic experiments. *Water Resources Research*, *49*(8), 5009–5020. https://doi.org/10.1002/wrcr.20384